Photoelectrochemical Properties of Sol-Gel Nb_2O_5 Films

DJALMA DE A. BARROS FILHO
Instituto de Física de São Carlos, Universidade de São Paulo,Caixa Postal 369, 13560-970, São Carlos, SP, Brasil

POMPEU P. ABREU FILHO
Departamento de Química, Universidade Estadual Paulista, Campus de Bauru, Caixa Postal 473, 17033-360, Bauru, SP, Brazil

U. WERNER
Institut für Neue Materialien, Im Stadtwald, Gebäude 43, D66-123 Saarbrücken, Germany

MICHEL A. AEGERTER
Instituto de Física de São Carlos, Universidade de São Paulo,Caixa Postal 369, 13560-970, São Carlos, SP, Brasil; and Institut für Neue Materialien, Im Stadtwald, Gebäude 43 D66-123, Saarbrücken, Germany

Abstract. Structural, optical, electro and photoelectrochemical properties of amorphous and crystalline sol-gel Nb_2O_5 coatings have been determined. The coatings are *n*-type semiconductor with indirect allowed transition and present an overall low quantum efficiency ($\phi < 4\%$) for UV light to electric conversion. The photoconducting behavior of the coatings is discussed within the framework of the Gärtner and Södergren models. Improvement can be foreseen if Nb_2O_5 coatings can be made of 10–20 nm size nanoparticles.

Keywords: sol-gel, Nb_2O_5, film, photoconductivity, photoelectrochemistry, semiconductor, solar cell

1. Introduction

Coatings made of semiconductor particles are particularly interesting for the development of solar energy storage and photochemical conversion devices, as electron and holes generated from band-gap excitation allow redox reactions. Small particles are synonymous of large surface area and the control of the chemical nature of their surface give the possibility to enhance the separation efficiency of the charge generated by light excitation carriers. Recently a novel approach of solar energy conversion using a photoelectrochemical cell has been reported [1]. In this method, 15 nm size TiO_2 particles are deposited on a conductive glass substrate to form a porous coating with high surface area. A monolayer of a ruthenium complex dye sensitizer allows a red shift of the UV range TiO_2 absorption spectrum toward the solar spectrum as well as an enhancement of the light absorption. Solar to electric conversion efficiency in the range of 7 to 12% has been reported.

In this paper we report on the sol-gel preparation of semiconducting Nb_2O_5 coatings and on the characterization of their structural, optical, photoconductive and photoelectrochemical properties. Besides their electrochromic properties [2], coatings realized with this material present analogous photoelectrochemical properties to TiO_2 coatings and may be an alternative for the developement of solar to electric conversion devices. The electro and photoelectrochemical behaviors of Nb_2O_5 thin films have been scarcely studied and mostly for amorphous coatings anodically electrodeposited [3–10]. These results are compared to those obtained with sol-gel films.

2. Experimental

The Nb_2O_5 coatings have been prepared by the sol-gel process and two different sol preparations have been tested. The first sol (Type I) consisted of a mixture of chloroalkoxide $NbCl_{5-x}(But)_x$ and *n*-butyl alcohol with a concentration of Nb equal to 1.49% M/M. The alkoxide was prepared by dissolving 11,5 g $NbCl_5$ purified by sublimation (CBMM-Brazil) in 40 ml dry *n*-butyl alcohol to which was added dry cyclohexane. After bubbling dry NH_3, amonium chloride was removed by filtration and the solvents evaporated under vacuum. In this process, all reactions and manipulations were carried out under dry nitrogen using standard Schlenk techniques. A second sol (Type II) was prepared by dissolving as received $0.2M$ $NbCl_5$ powder (CBMM) in $0.28M$ butanol and $0.05M$ acetic acid. The solution was then sonocatalized for a few minutes (Sonicator W385 Heat System Ultrasonic, 20 kHz) resulting in a transparent and viscous solution stable for several months at room temperature. The main precursors are also probably chloroalkoxides of the type $NbCl_{5-x}(OBut)_x$. This sol is easier to prepare than the first one.

The coatings have been deposited by dip coating technique at a withdrawal speed of 12 cm/min. on ITO coated glass (Asahi Glass (14 Ω/□) or Donelly Corp.), previously cleaned and rinsed with bidistilled water and ethanol. They were dried in air at 25°C for 5 min and then heated up to 350°C and held at this temperature for 5 min. The whole process was repeated in order to increase the thickness of the coatings. The final coatings were heat treated in air at the desired temperature ($450 < T < 600$°C) for 2 h. They were transparent and homogeneous. Xerogels and precipitates have also been prepared with Type II sol [11].

The thickness of the coatings (d) has been determined using a Taylor Hobson Talystep; a single layer is typically 40 ± 4 nm and ~100 nm thick for Types I and II sol respectively.

The UV absorption spectra of the films were measured with a Cary 17 spectrometer with films submitted to the same heat treatment procedure but deposited on Suprasil fused quartz slide.

The photoelectrochemical response of the films has been determined using an electrochemical cell having a fused quartz window for light excitation from a calibrated Bausch and Lomb system comprising a 100 W Xe lamp coupled to a high intensity monochromator (band width 16 nm). The monochromatic light output $I_{h\upsilon}$ was quantitatively calibrated using a Labmaster/Fieldmaster Coherent LM 2 and LM-2UV detector down to 250 nm. The action spectrum was measured in reference to a saturated calomel electrode (SCE) and a Pt foil as counter electrode. The electrolyte was an aqueous solution of $0.2M$ $LiClO_4$ (pH = 5.9) purged with dry N_2 gas. The measurements were performed using a computerized PAR Model 273A potentiostat.

3. Results and Discussion

X-ray diffraction of xerogels obtained with Type II sol, heat treated between 400 and 600°C during 10 min, show that the material is amorphous at 400°C and starts to crystallize at ~450°C [2]. Similar results have been obtained with xerogels obtained with Type I sol. The diffraction peaks observed up to 600°C correspond to the TT structure, which is not a stoichiometric niobium pentoxide, as some oxygen atoms are replaced by monovalent species (vacancies, OH^-, etc.). The compound should be noted $Nb_2(OX)_{5+n}$ [12]. This evolution was confirmed by DSC, DTA, SEM and infrared measurements [13].

The texture of the films prepared was studied by scanning electron microscopy (SEM) with coatings prepared with Types I and II sols and AFM microscopy with a series of coatings prepared with Type II sol only. Due to its poor resolution, the first technique does not allow any safe conclusion. Figure 1 shows two AFM images of coatings. Although some artifacts are seen (e.g., horizontal stripes), one clearly recognizes a change in the surface structure from a rather smooth surface for the 400°C amorphous film (Fig. 1(b)) to a probably porous surface built with well defined shaped clusters of large particles (size ~500 nm) surrounded by smaller particles (size ~100 nm) for the 600°C crystalline film (Fig. 1(a)). Unfortunately, no AFM measurements are yet available for coatings prepared with Type I sol. However, as SEM micrographs did not present a definite texture for both type of coatings, it is expected that the texture of Type II coatings observed at higher resolution should not be drastically different than that presented in Fig. 1.

Absorption spectra of 1 layer 40 nm thick films prepared with Type I sol and heat treated at 400, 500, 560 and 600°C are shown in Fig. 2. Similar behavior has been obtained for thicker films. The films exhibited a good spectral homogeneity (within 2 cm^2 area). The wavelength dependence of the absorption coefficient is typical of amorphous or polycrystalline semiconducting materials. The high energy side can be fitted to the Tauc law $(\alpha h\upsilon)^{1/2} = A(h\upsilon - E_g)$ [14]

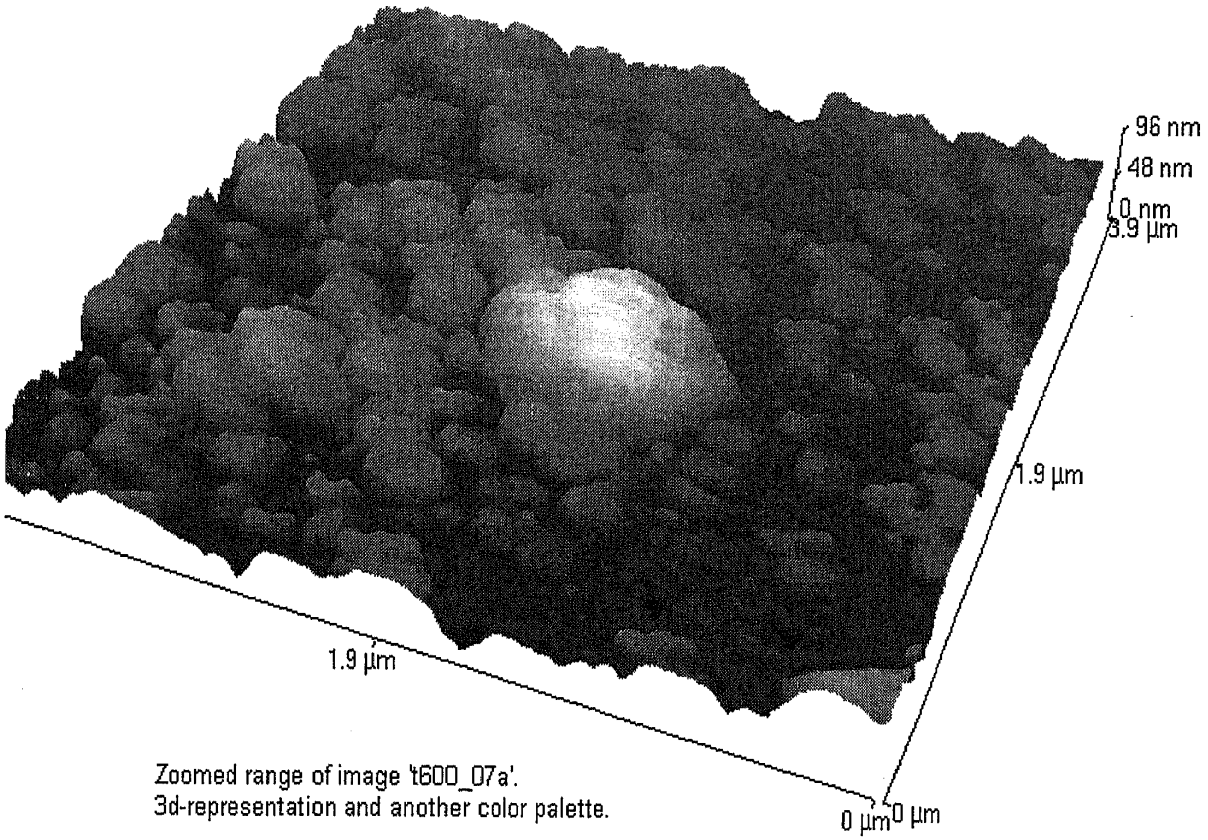

(a)

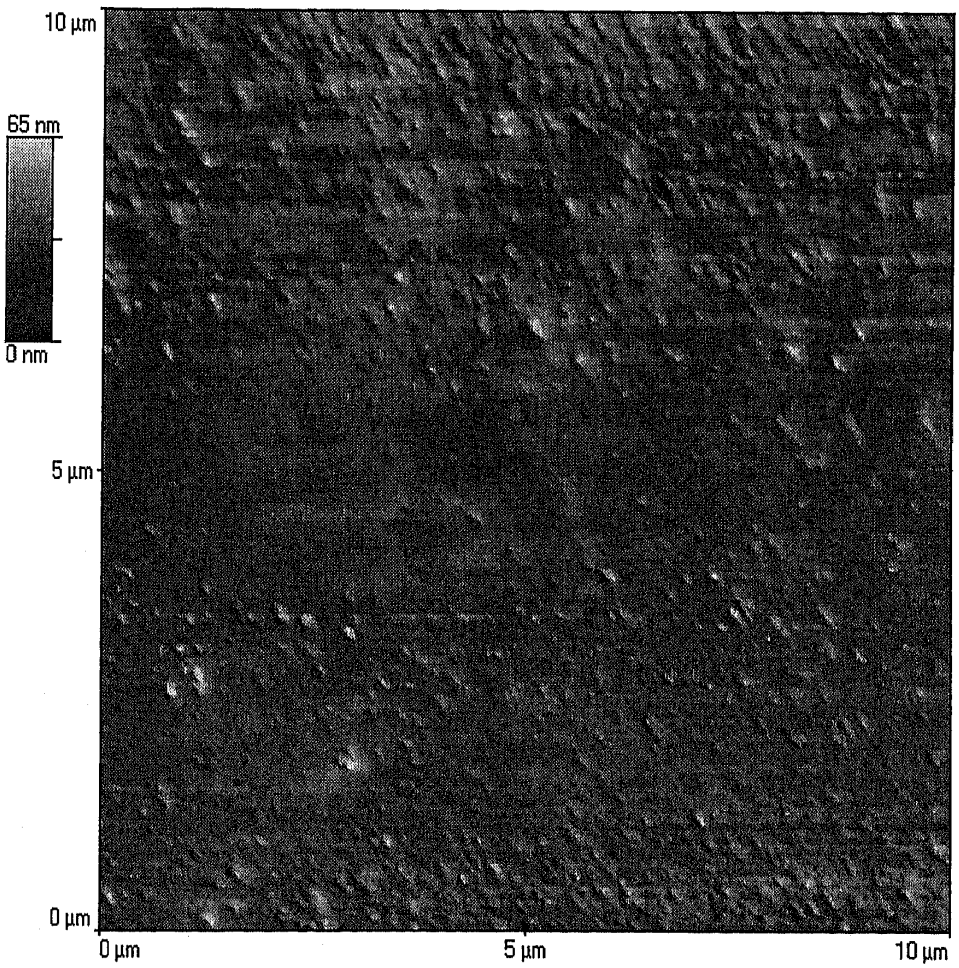

(b)

Figure 1. AFM images of Nb_2O_5-coating surface prepared with Type II sol 100 nm thick heat treated at (a) 600°C/2 h (crystalline); (b) 400°C/2 h (amorphous).

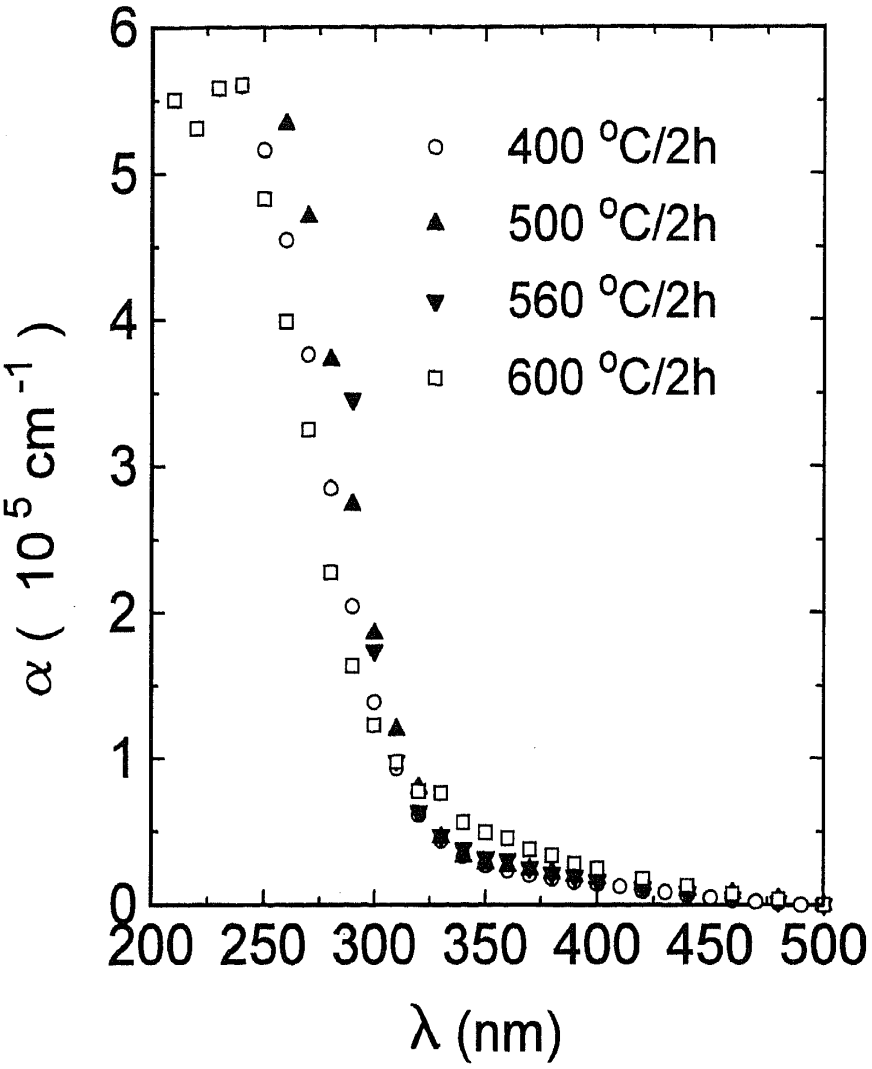

Figure 2. Optical absorption spectra of 40 nm Nb_2O_5 films prepared with Type I sol, deposited on fused silica substrate and heat treated during 2 h at 400°C (○), 500°C (▲), 560°C (▼) and 600°C (□).

valid for indirect allowed transitions (Fig. 3). The values of the optical band gap, E_g, determined by the intersection of the straight line with the abcissa are given in Table 1. E_g is sligthy smaller (0.1 eV) for the amorphous material. In all spectra the low energy tail, which is commonly observed in most amorphous and polycrystalline semiconductors, reflects the presence of sub-band gap optical transitions due to electrons originated in states in the mobility gap. They fit the Urbach rule [15] $\alpha = A \exp[a(h\upsilon - E_0)/kT]$ where A, a and E_0 are empirical constants.

Table 1. Band gap energy, E_g, determined optically and electrochemically with 40 nm thick niobia coating heat treated at different temperatures.

Thickness (±2 nm)	~40	~40	~37
Heat treatment (°C/2 h)	400	500	600
Optical band gap (±0.1 eV)	3.4	3.5	3.5
Band gap (el. chem.) (±0.1 eV)	3.37	3.41	3.39

The band gap can also be determined photoelectrochemically by measuring the action spectra of the films. Typical spectra measured and corrected for constant light irradiation intensity from the eletrolyte side (EE configuration) are shown in Fig. 4 for single layer 40 nm thick crystalline coatings heat treated at 560°C/2 h as a function of the anodic polarization. These spectra present a broad maximum with a long tail at low photon energy and a cut-off at high energy where the value of the current drops practically to zero. The current intensity increases with the value of the anodic potential. The shape of these spectra measured for films densified between 400 and 600°C is essentially the same. When the temperature increases, it slightly narrows and the maximum of the current increases and slightly shifts to lower wavelength. For all wavelength the current (i) was found to vary linearly with the light intensity (measured up to $I_{h\upsilon} \cong 50$ μW/cm^2) within the polarization range $0 < E < 1$ V. A plot of $(ih\upsilon/I_{h\upsilon})^{1/2}$ vs $h\upsilon$ [16] gives a straight line confirming the results obtained

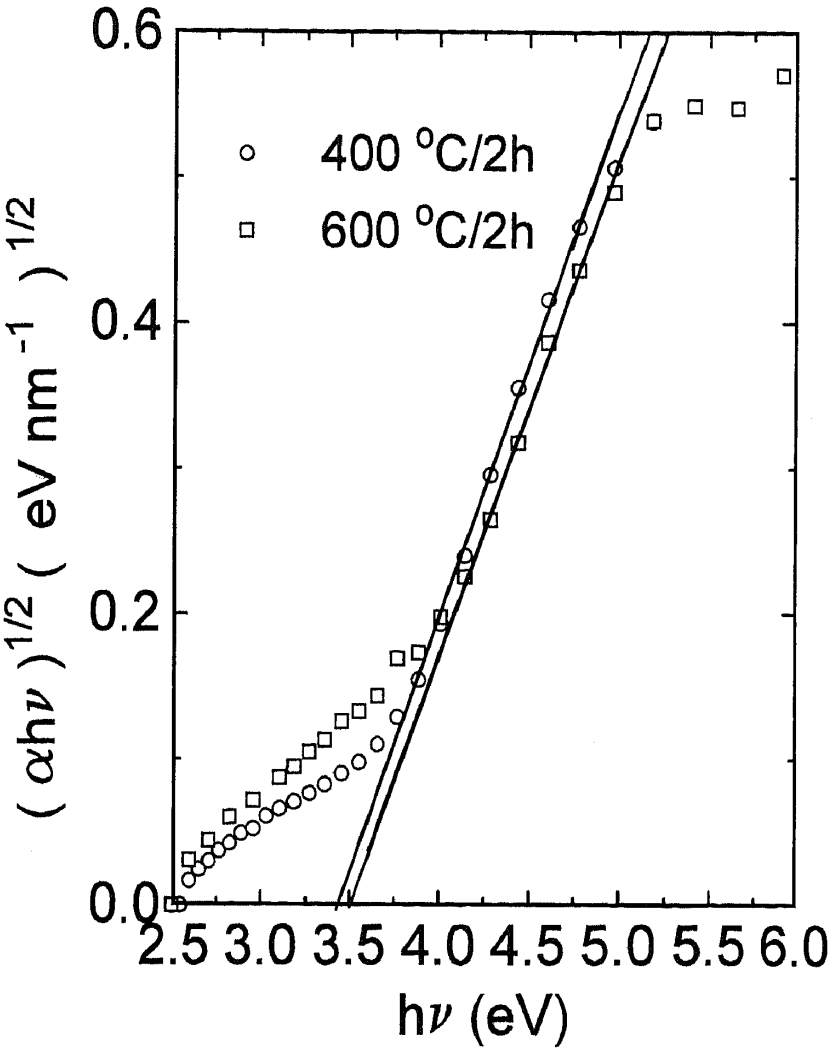

Figure 3. Fit of the results of Fig. 2 to the Tauc law $(\alpha h\upsilon)^{1/2} = A\,(h\upsilon - E_g)$; (○) amorphous film, 400°C/2 h, (□) crystalline film, 600°C/2 h.

optically (Fig. 5). The values of E_g agree with those of the literature obtained for amorphous film deposited electrochemically on metallic Nb: (3,35 ± 0,05 eV ($20 < d < 250$ nm) [8], ~3,18 eV ($d \sim 12$–52 nm) [9] and 3,4 eV [6]. Excitation in the low energy tail of the optical absorption does not seem to contribute to the electronic current.

The quantum efficiency ϕ for light to electric conversion is defined as the ratio of the number of electrons of the photocurrent n_e to the number of incident photons n_f

$$\phi = \frac{n_e}{n_f} = \frac{hc}{e\lambda}\frac{i}{I_{h\upsilon}} \qquad (1)$$

Figure 6 shows typical ϕ spectra determined from the action spectra of the films measured with a fresh electrolyte at 0 V polarization and corrected for the wavelength dependence of the light intensity of the monochromatic excitation system (including the electrolyte). Several interesting conclusions can be drawn:

a) the maximum values of ϕ are all <3% (Fig. 6), a value smaller than those determined for TiO_2 films built with nanoparticles ($\phi \sim$<20%) [17].
b) the overall values of ϕ increase and the maximum shifts slightly to higher energy with the degree of crystallization of the coatings (Fig. 6(b)).
c) the values of ϕ increase with the anodic polarization (Fig. 4).
d) the photocurrent (or ϕ) drops drastically at high photon energy, in contradiction with the Gerischer [18] and Gärtner [19] models which predict that the photocurrent should increase with the photon energy up to a steady value unless there is a surface recombination (photon absorption closer to the material-electrolyte interface) leading to a decrease of i or ϕ.
e) the overall values of ϕ decrease substantially if the coatings are left in the electrolyte for long period of time. This is due in part to a dissolution of the coatings which turns the electrolyte absorbant below 280 nm, but also to the growth of an optical absorbant but not photoconducting layer

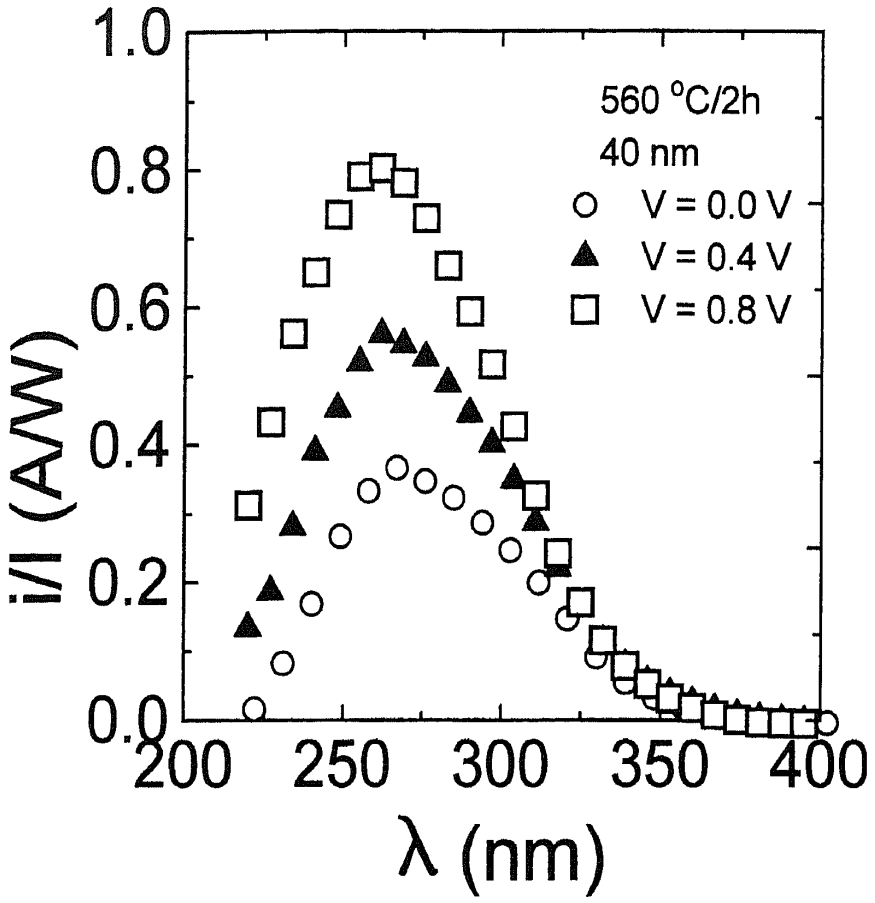

Figure 4. Corrected action spectra of a 40 nm thick Nb_2O_5 coatings prepared with Type I sol and heat treated at 560°C/2 h measured with anodic polarization of 0 V (○), 0,4 V (▲), 0,8 V (□) vs SCE.

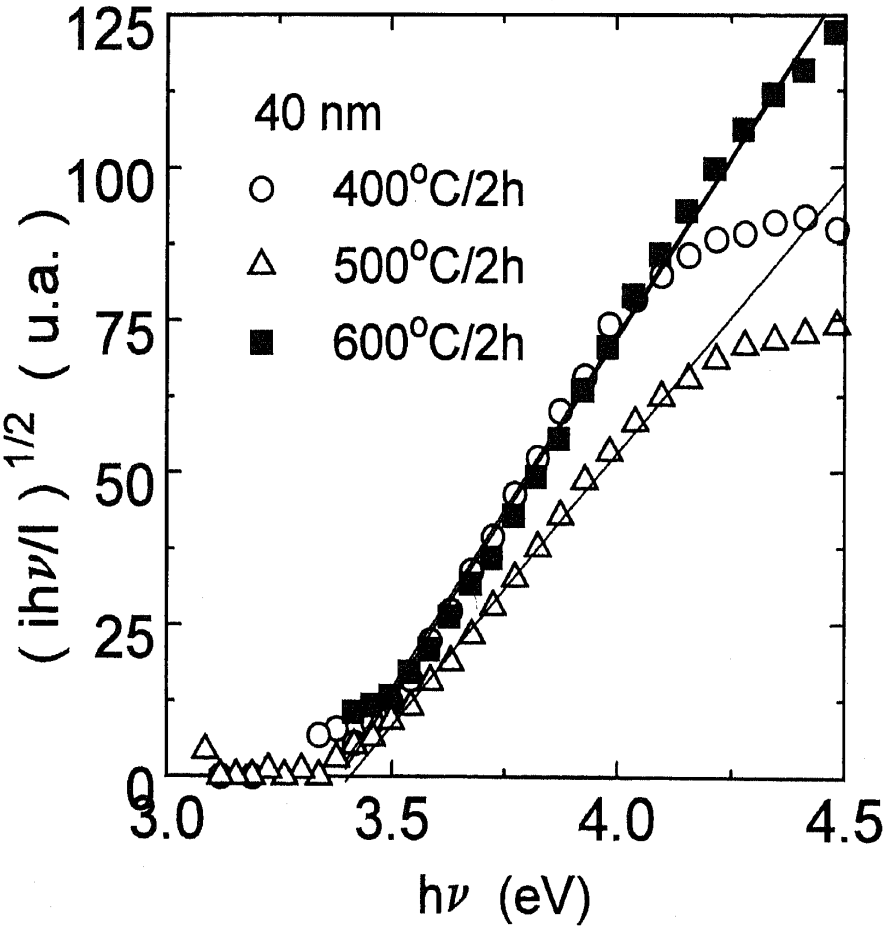

Figure 5. $(ih\upsilon/I_{h\upsilon})^{1/2}$ vs $h\upsilon$ plot for 40 nm thick Nb_2O_5 coating prepared with Type I sol; heat treatment 400°C/2 h (○), 500°C/2 h (△), 600°C/2 h (■).

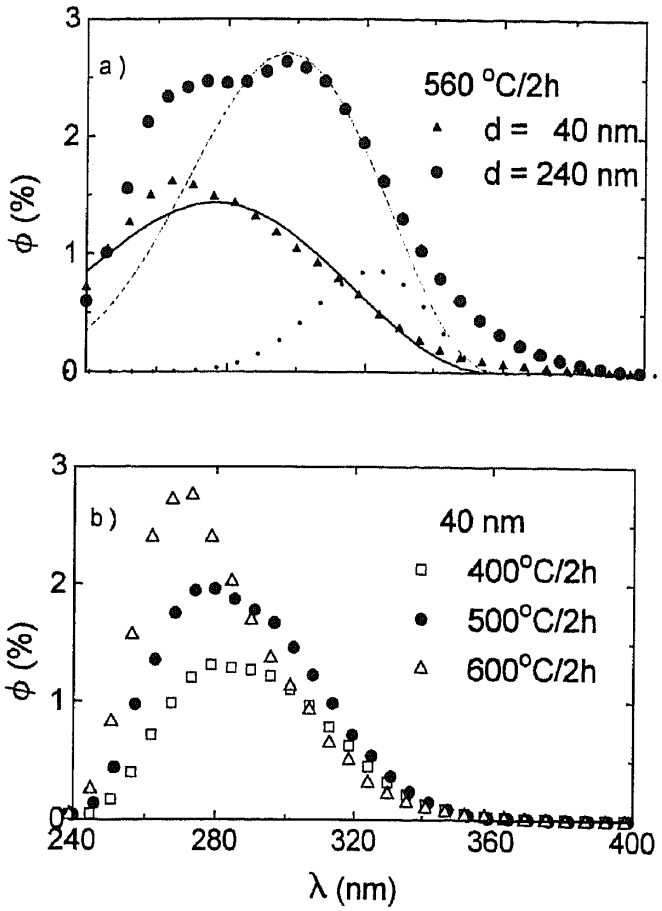

Figure 6. Quantum efficiency ϕ (%) of Nb_2O_5 films prepared with Type I sol, heat treated during 2 h, calculated for a constant spectral light irradiation intensity: (a) 40 (▲) and 240 nm (●) thick heat treated at 560°C/2 h; (----) best fit with $L = 1.5$ nm and $d = 40$ nm (real thickness of the film), (—) best fit with $L = 5.5$ nm and $d = 80$ nm (effective thickness of the active layer), (···) fit with $L = 5.5$ nm and $d = 240$ nm (real thickness of the film); (b) 40 nm thick: (□) 400°C, (●) 500°C, and (△) 600°C.

at the film-electrolyte interface of still unknown origin.

f) the values of ϕ increase only slightly with the thickness of the coating and the position of the maximum is practically not altered (Fig. 6(a)).

These spectra are better explained using a model idealized first by Hodes et al. [20] for porous films made of CdS and CdSe nanoparticles and recently calculated by Södergreen et al. [21]. The fits of the quantum efficiency for light excitation from the electrolyte side (EE configuration) and using Eq. (10) of Ref. [21] are also shown in Fig. 6(a). For the one layer coating shown in the figure the fit was done using its real thickness (40 nm) and an electron diffusion length $L = 1.5$ nm. The agreement is satisfactory. The L value is much smaller than that found for TiO_2 nanoparticles coating, $L \simeq 800$ nm [21]. However, for thicker films and similar L values no good fit can be obtained using the real value of the thickness (Fig. 6(a)). The best fit for the 240 nm coating (6 layers) was obtained with $d = 80$ nm and $L = 5.5$ nm.

These results may be explained by the following considerations: the AFM image (Fig. 1(a)) shows that the external region of the film is made of small and large particles arranged to give a porous structure where the electrolyte can penetrate. The current, i, generated by the UV light irradiation, is due to electrons which have been separated from their corresponding holes, a phenomenon which can only occur for electron-hole pairs created either within a thin depletion layer of the large particles (those generated in the bulk of the particles will easily recombine) or within the nanoparticles whose surface has been modified by the electrolyte [20, 21]. Inspection of Fig. 1(a) shows that the concentration of these particular pairs must be small leading to small values of the quantum efficiency ϕ (<4%) and electron diffusion length. The reasonable fit obtained with the Södergren model for the 40 nm thick coatings (Fig. 6(a)) are in agreement with these assumptions. The model applied to the results obtained with thicker films predicts that the maximum of ϕ should lay at a wavelength corresponding to $\alpha = d^{-1}$, i.e., at a much longer wavelength and that the current should increase more as most of the photons will be absorbed. This is not observed experimentally and the best fit was obtained using an active thickness of ~80 nm. This is an indication that the thick films are probably composed of an external porous layer of such thickness (where the model applies) and that the region below, down to the ITO coating, is mainly inactive in the sense that the electron-hole pairs generated by the UV photons essentially recombine and do not contribute to the current. This occurs either because this region is too dense (no penetration of the electrolyte) or it does not contain small enough particles; both phenomena may result from the successive heat treatments realized for the coating densification. If this rationale is correct, considerable improvement are expected if Nb_2O_5 coatings can be built with 10–20 nm size nanoparticles, as it was shown for TiO_2 coatings, and Nb_2O_5 coatings will be an alternative to build efficient and cheap solar cells.

However, at the present stage of knowledge, it cannot be discarded that other phenomena , lowering the efficiency of the cell, may also play a role such as isoenergetic or inelastic charge transfer at the eletrolyte-semiconductor interface, effect of illumination with

charge transfer to oxidised species, presence of surface states allowing surface recombination, etc.

Conclusion

Structural, optical, electro and photoelectrochemical properties of amorphous and crystalline sol-gel Nb_2O_5 coatings have been determined. The results indicate that these films are *n*-type semiconductor with a low quantum efficiency for light to electric conversion in the UV spectral range. For thin film (<50 nm) the results are explained quantitatively within the framework of Södergren's model [21]. For thicker films, apparently, the photo current is generated only in a small external region of the film, ~80 nm thick, in contact with the electrolyte. The low Nb_2O_5 efficiency ($\phi < 3\%$ compared to 20% for TiO_2 coating made with nanocrystalline particles) is therefore probably due to the particular structure of our coatings. Considerable improvement is expected if Nb_2O_5 coatings can be made with nanocrystalline particles 10–20 nm size which we believe is a sine qua non condition. Research are in progress in these directions in order to improve the photoelectrochemical properties of niobia coatings and to build solar light to electric conversion cells of high efficiency.

Acknowledgment

Research sponsored by FAPESP, CNPq, FINEP and FUNDUNESP. The authors gratefully acknowledge the CBMM (Brazil) by the $NbCl_5$ supplied.

References

1. M. Graetzel, in Nanocrystallize Thin-Film PV Cell, MRS Bulletin XVIII **10**, 61 (1993).
2. M.A. Aegerter, C.O. Avellaneda, and A. Pawlicka, this Proceedings.
3. L. Young, Trans. Faraday Soc. **52**, 502 (1956).
4. D. Stützle and K.E. Heusler, Z. Phys. Chem. N. Flge **65**, 201 (1969).
5. K.E. Heusler and J.W. Schulze, Electrochim. Acta **20**, 237 (1975).
6. P. Clechet, J. Mertin, R. Oliver, and C. Vallouy, C.R. Acad. Sci. C **282**, 887 (1976).
7. F.D. Quarto, C. Sunseri, and S. Piazza, Ber. Bunsen. Phys. Chem. **90**, 549 (1986)
8. F. Di Quarto, S. Piazza, R. d'Agostino, and C. Sunseri, J. Electroanal. Chem. **228**, 19 (1987).
9. C.K. Dyer and J.S.L. Leach, Electrochim. Acta **20**, 151 (1975).
10. C.V.V. d'Alkaine, L.M.M. de Souza, and F.C. Nart, Corrosion Science **34**, 109 (1992)
11. A. Pawlicka, M. Atik, and M.A. Aegerter, J. Mat. Sci. Let. (Accepted).
12. E.I. Ko and J.G. Weissman, Catalysis Today **8**, 27 (1990).
13. A. Pawlicka, M. Atik, and M.A. Aegerter, Submitted to J. Electrochem. Soc.
14. J. Tauc, *Amorphous and Liquid Semiconductor* (Plenum Press, New York, 1974).
15. F. Urbach, Phys. Rev. **92**, 1324 (1953).
16. M.A. Butler, J. Applied Physics **48**, 1914–1920 (1977).
17. A. Hagfeldt, U. Björkstén, and S.E. Lindquist, Solar En. Mat. and Solar Cells **27**, 293 (1992).
18. H. Gerischer, Adv. Electrochem. Eng. **1**, 139 (1969); J. Electrochem. Soc. **113**, 1174 (1966); *Physical Chemistry: An Advanced Treatize* (Acad. Press, New York, 1970), vol. 9A.
19. W.W. Gärtner, Phys. Rev. **116**, 84 (1959).
20. G. Hodes, I.D.J. Howell, and L.M. Peter, J. Electrochem. Soc. **139**, 3136 (1962).
21. S. Södergren, A. Hagfeldt, J. Olsson, and S.E. Lindquist, J. Phys. Chem. **96**, 5552 (1994).